Trimming the UCERF2 Hazard Logic Tree

by Keith A. Porter, Edward H. Field, and Kevin Milner

INTRODUCTION

Assessing Which Sources of Hazard Uncertainty Matter

The Uniform California Earthquake Rupture Forecast 2 (UCERF2) is a fully time-dependent earthquake rupture forecast developed with sponsorship of the California Earthquake Authority (Working Group on California Earthquake Probabilities [WGCEP], 2007; Field *et al.*, 2009). UCERF2 contains 480 logic-tree branches reflecting choices among nine modeling uncertainties in the earthquake rate model shown in Figure 1. For seismic hazard analysis, it is also necessary to choose a ground-motion-prediction equation (GMPE) and set its parameters. Choosing among four next-generation attenuation (NGA) relationships results in a total of 1920 hazard calculations per site. The present work is motivated by a desire to reduce the computational effort involved in a hazard analysis without understating uncertainty. We set out to assess which branching points of the UCERF2 logic tree contribute most to overall uncertainty, and which might be safely ignored (set to only one branch) without significantly biasing results or affecting some useful measure of uncertainty. The trimmed logic tree will have all of the original choices from the branching points that contribute significantly to uncertainty, but only one arbitrarily selected choice from the branching points that do not.

Risk analyses that use the trimmed tree should produce approximately the same results as those that use the full tree. Risk, as used here, refers to the relationship between some undesirable outcome and its likelihood of occurrence, typically from some particular decision-maker's perspective. Risk can be measured in terms of an uncertain quantity of loss, such as the relationship between future earthquake-related repair costs to a particular asset or group of assets and the probability of exceeding that cost, or in terms of a scalar measure of that relationship, such as the expected annualized value of that repair cost. Risk professionals commonly use both continuous and point measures. Insurers, for instance, commonly make reinsurance purchasing decisions using loss exceedance curves (which relate insured loss to exceedance frequency), and set insurance premiums based on a point value related to the curve, especially the expected annualized loss (EAL).

Risk information is typically a prerequisite for risk management—for making decisions to reduce or transfer the risk. The particular risk-management decision in question helps to determine which risk metrics should be estimated. UCERF2 affects a variety of risk-management decisions, such as engineering design requirements, insurance pricing and reinsurance purchases, and public policy about life safety and economics at a variety of geographic levels. This work examines UCERF2 from a statewide perspective, considering its economic implications, while acknowledging that other perspectives are also worth exploring.

For the reader unfamiliar with UCERF2, we briefly review the meaning of each branching point (often called epistemic uncertainty).

- ***Fault models*** specify the geometry of larger, more active faults.
- ***Deformation models*** refer to assigning a slip rate, an aseismic slip factor, and their uncertainties, to each fault section.
- ***Magnitude–area relationships*** give the average magnitude for a given rupture area.
- ***Segmentation for type-A faults*** imposes rupture boundaries, but might be a bad approximation; for this reason, an alternative, unsegmented approach is also considered.
- ***Fault-slip rates within the segmented model on type-A faults***. The alternatives comprise an *a-priori* (consensus) rate model and a version to match observed long-term slip rates.
- ***Type-B earthquake rate models: connect more type-B faults?*** This refers to modeling nearby type-B faults as capable of producing larger earthquakes.
- ***Type-B fault b-values***. The slope of the Gutenberg-Richter component of the magnitude–frequency relationship for type-B faults can take on the values 0.0 and 0.8.
- ***Recurrence models and aperiodicity***. The alternatives are a Poisson model, an empirical model that accounts for earthquake rate changes over the last 150 years, and a Brownian passage time (BPT) model with uncertain aperiodicity to reflect elastic rebound.
- ***Ground-motion-prediction equation***. Though not an element of UCERF2, GMPEs are required for a probabilistic seismic hazard analysis. Figure 2 illustrates the difference between two GMPEs for a particular set of parameter values.

Each uncertainty has scientific relevance and scientific value in its resolution. There are also practical values to consider. For example, to an insurer, greater uncertainty in risk means higher losses are more likely. Insurers buy reinsurance based on large, rare events, often the loss with 1/250 chance of occurrence per year. Greater uncertainty means greater reinsurance cost. Figure 3 illustrates two loss-exceedance curves for the same portfolio with differing uncertainty. The EAL may be the same, but the 250-year losses are not. Thus, there can be a strong financial incentive to reduce uncertainty as cost-effectively as possible.

doi: 10.1785/0220120012

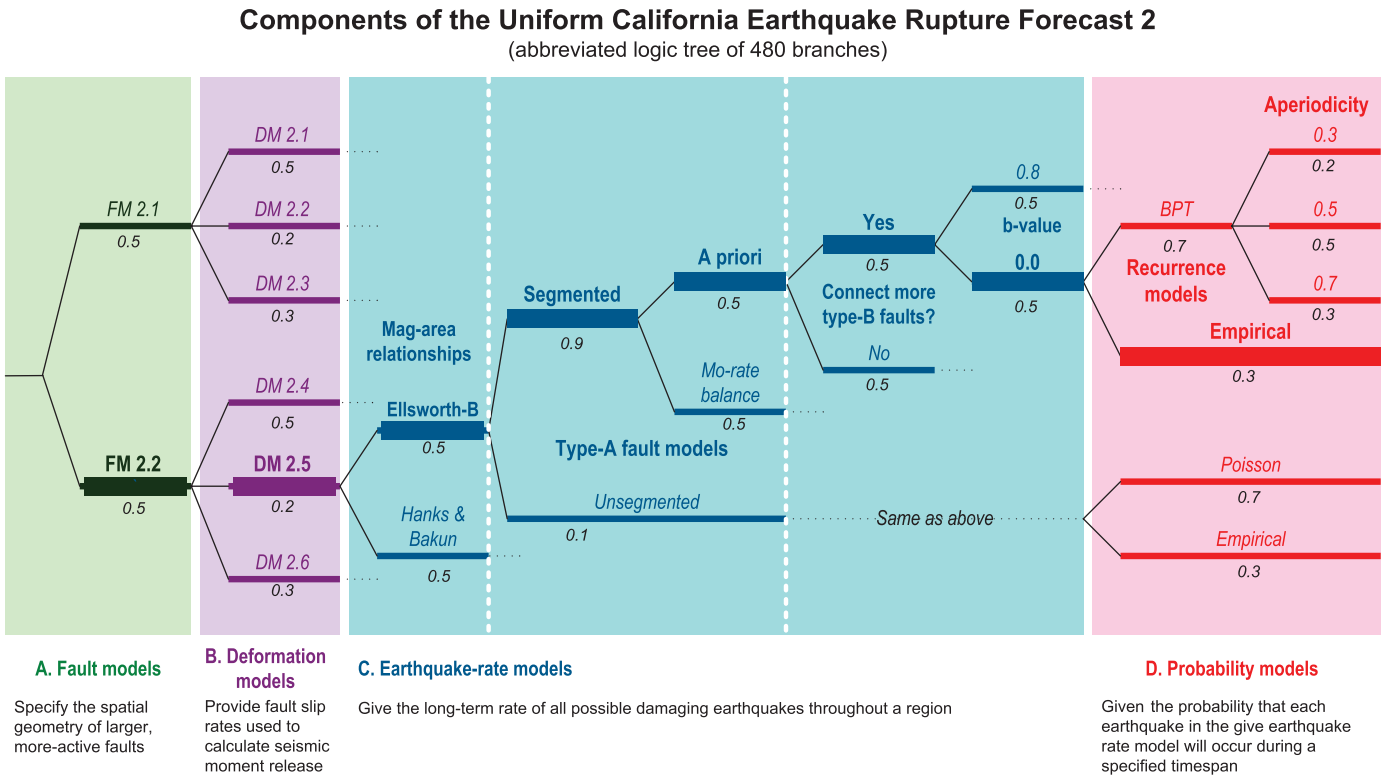

▲ **Figure 1.** Branches of the UCERF2 logic tree (after WGCEP, 2007). Dotted lines (…) indicate that the tree continues parallel to the branches that are shown, but that these branches are omitted from the figure for clarity. Black numbers below branches are the branch weights.

Propagating each uncertainty through hazard and risk analyses also carries a computational cost, and can be prohibitively time-consuming for large portfolios or maps. We acknowledge but do not address here the relative scientific importance of resolving UCERF2's epistemic uncertainties. Instead, we explore the relative practical importance of the epistemic uncertainties by testing the sensitivity of a particular risk metric to each branching point.

There is a wide variety of potentially useful metrics of sensitivity, and substantial literature on the general topic. We will summarize only a few prior works. Cornell and Vanmarcke (1969) examined the sensitivity of the PGA hazard curve to event magnitude. Youngs and Coppersmith (1985) examined the sensitivity of the full seismic hazard curves at selected sites to variations in recurrence models and parameters that incorporate fault slip rates. Rabinowitz *et al.* (1998) explored the sensitivity of PGA at a single site to the epistemic uncertainties in the hazard logic tree. Akinci *et al.* (2009) examined the sensitivity of hazard maps of the Central Apennines of Italy to the choice of rupture probability models and aperiodicity parameter for a BPT model.

We could examine the uncertainties' effect on uniform seismic hazard maps such as those underlying the American Society of Civil Engineers' (ASCE) seven maximum considered earthquake (MCE) maps, which are of 5%-damped spectral acceleration response at various periods (0, 0.2 sec, 1 sec, etc.) with 2% exceedance probability in 50 years (ASCE, 2005). Alternatively, we could examine the effect on the maps of risk-targeted maximum considered earthquake (MCE_R) ground motions that produce nominally uniform collapse risk (ASCE, 2010). One challenge is whether, and how, to decide which locations matter.

Grossi (2000) examines how EAL and a "worst-case loss" for Oakland, California, vary when one changes any of several model parameters, namely the earthquake rupture forecast (USGS versus a proprietary model), the GMPE (two choices are considered), soil (the choice is a single uniform National Earthquake Hazards Reduction Program (NEHRP) site class or varying soil by location), and the fragility model.

Like Grossi (2000), we use a risk metric, focusing on the sensitivity of societal risk to individual uncertainties in the hazard logic tree. Two downsides to this approach are that results may differ between portfolios, and that new uncertainties, especially vulnerability, are introduced. We considered several risk metrics, and like Grossi (2000) chose EAL, which here means the average ground-up repair costs, per year, to the portfolio in question. We examine a portfolio of the estimated quantity of single-family woodframe dwellings in California, partly for convenience and partly because of its relevance to UCERF2's principal sponsor, the California Earthquake Authority. The portfolio was developed from the HAZUS-MH estimated inventory of California construction. Next we detail the tornado-diagram analysis, the development of the portfolio, and the method for calculating EAL.

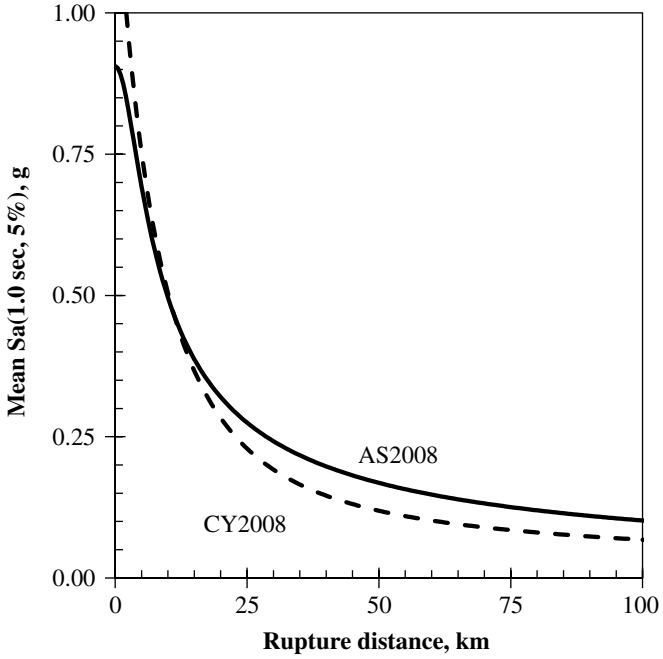

▲ **Figure 2.** NGA relationships can significantly differ. For example, Abrahamson and Silva (2008) tends to produce higher median 1-sec, 5%-damped spectral acceleration response than does Chiou and Youngs (2008) for distances greater than about 10 km, given an M 7 event, 5 km to top of rupture, V_{S30} of 330 m/sec, and 500 m depth to 1 km/sec shearwave velocity.

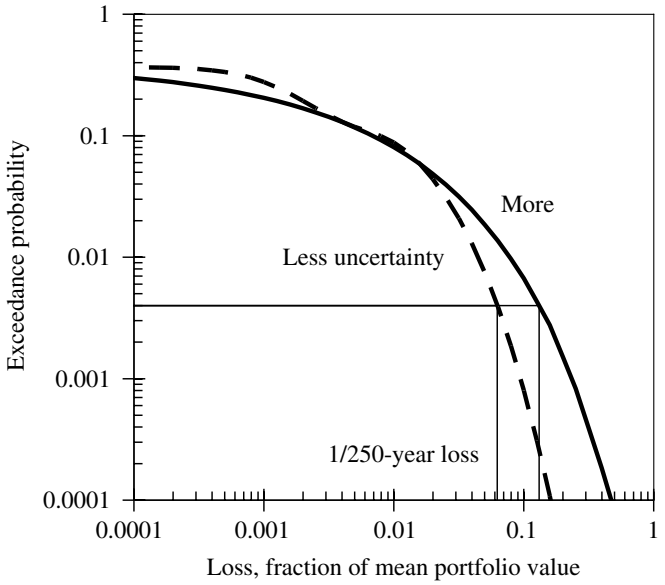

▲ **Figure 3.** More uncertainty in risk translates to higher loss at low exceedance probabilities which, for an insurance company, demands more reinsurance and more expense. (Portfolio value is uncertain, hence "mean" in the x-axis label.)

TORNADO DIAGRAMS

Earthquake engineers sometimes employ this graphical technique from the field of decision analysis to test the sensitivity of seismic risk to major uncertain variables (e.g., Porter *et al.*, 2002; Multihazard Mitigation Council [MMC], 2005). The technique is useful for examining the sensitivity of a scalar deterministic function of uncertain input variables. It depicts the effect on the function by varying each uncertain input individually, while keeping the other parameter values fixed at some best-estimate or baseline value.

That is, one is interested in some function $Y = f(X)$, where Y is an uncertain scalar variable, X is a vector of one or more scalar uncertain input variables, and f is a deterministic function. To explore which component of X strongly affects Y, one evaluates a series of $Y_i = f(X_i)$, where X_i denotes a sample vector of X (i.e., given values of each component of X). In the following, n denotes the number of components or elements of X, $X^{(i)}$ denotes the ith component of $X (1 \le i \le n)$, $E[X]$ denotes the expected value of X, that is the vector of X where every component is set to its average or baseline value, $E[X^{(i)}]$ is the baseline value of component i of the vector X, $X^{(i)}_{\mathrm{LB}}$ denotes a lower-bound value of $X^{(i)}$ (can be either qualitatively defined or, optionally, a specified percentile, such as the 10th), $X^{(i)}_{\mathrm{UB}}$ denotes an upper-bound value of $X^{(i)}$ (likewise, either a qualitative value or a specified upper percentile), and $\{\bullet\}$ denotes a vector composed of the elements inside the brackets. Then one evaluates $Y_0, Y_1, \ldots Y_{2n}$ as follows:

$$
\begin{aligned}
Y_0 &= f(E[X]) \\
Y_1 &= (\{X^{(1)}_{\mathrm{LB}}, E[X^{(2)}], \ldots E[X^{(n)}]\}^T) \\
Y_i &= f(\{E[X^{(1)}], \ldots X^{(i)}_{\mathrm{LR}}, \ldots E[X^{(n)}]\}^T) \qquad 1 < i < n \\
Y_n &= f(\{E[X^{(1)}], E[X^{(2)}], \ldots X^{(n)}_{\mathrm{LB}}\}^T) \\
Y_{1+n} &= f(\{X^{(1)}_{\mathrm{UB}}, E[X^{(2)}], \ldots E[X^{(n)}]\}^T) \\
Y_{i+n} &= f(\{E[X^{(1)}], \ldots X^{(i)}_{\mathrm{UB}}, \ldots E[X^{(n)}]\}^T) \qquad 1 < i < n \\
Y_{2n} &= f(\{E[X^{(1)}], E[X^{(2)}], \ldots X^{(n)}_{\mathrm{UB}}\}^T). \qquad (1)
\end{aligned}
$$

The sensitivity of Y to component $X^{(i)}$ is indicated by the difference (or "swing"):

$$\mathrm{Swing} = |Y_i - Y_{i+n}|. \qquad (2)$$

To create the diagram, one sorts the X components in decreasing swing, and creates a horizontal bar chart where the horizontal axis measures Y, and each horizontal bar corresponds to one of the X components. The ends of the topmost bar are placed at Y_i and Y_{i+n} for the component with the largest swing, the next higher bar shows Y_j and Y_{j+n} for the component j with the next-largest swing, etc. A vertical line is drawn intersecting the horizontal axis at Y_0. The diagram resembles a tornado in profile, and shows which input variables probably matter most to the uncertainty in Y and which might be ignored.

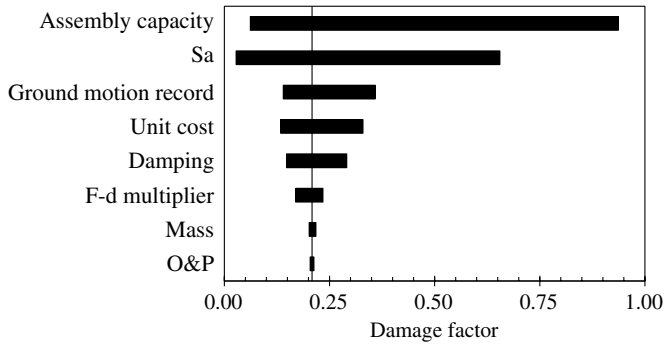

▲ **Figure 4.** Sample tornado diagram (Porter *et al.*, 2002). In the figure, "assembly capacity" refers to the demand at which a building assembly enters a specified damage state. Sa denotes the maximum experienced value of 5%-damped elastic spectral acceleration response at the building's estimated small-amplitude fundamental period of vibration. "F–d multiplier" refers to uncertainty in the *X* and *Y* values of the force-deformation relationship of structural components. "O&P" refers to contractor overhead and profit, a factor applied to the contractor's direct cost that relates the owner's costs to the contractor's.

A sample is shown in Figure 4. It shows that the variable called damage factor is most sensitive to uncertainty in a variable called assembly capacity. With all other input variables (S_a, ground motion record, etc.) set to their baseline value, uncertainty in assembly capacity can make the damage factor as low as 0.07 or as high as 0.94. Assembly capacity and S_a seem to dominate uncertainty in damage factor, implying that uncertainty in the other variables might be ignored for purposes of estimating damage factor.

ANALYSIS

Estimating the Portfolio of Interest

No actual enumeration of the California building stock exists, there being no authority responsible for compiling one. The HAZUS-MH portfolio instead is based on population and employment statistics (see National Institute of Building Sciences [NIBS] and Federal Emergency Management Agency [FEMA], 2009, for details). To summarize (and oversimplify), the HAZUS-MH model encodes statistics or engineers' judgment of the square footage required for each resident or worker, along with the per-square-foot value and building-type distribution by economic sector and several categories of residential construction. Thus, the HAZUS-MH model estimates the replacement cost of buildings for a given structure type and census block as follows:

$$V = \sum_o P(o) \cdot A(o) \cdot T(o) \cdot R, \tag{3}$$

where o is an index of occupancy category, P denotes the number of people in the census block in occupancy category o, A denotes the estimated average square footage per person in that occupancy category, T is the fraction of building area of the given occupancy category constructed of the structure type of interest, and R is the estimated replacement cost per square foot for that structure type.

The HAZUS-MH (2009) software provides these parameter values in a database; we compiled the quantities for single-family dwellings and woodframe buildings of less than 5000 square feet. The total estimated replacement cost of these California buildings is \$1.6 trillion. The statewide total for all residential buildings is \$2.1 trillion; for buildings of all classes it is \$2.7 trillion. The portfolio considered here represents 60% of all California buildings by replacement cost.

Evaluating the Expected Annualized Loss

We developed software called the Portfolio EAL Calculator to estimate this risk metric as part of the OpenRisk effort described by Porter and Scawthorn (2007, 2009). The calculator is part of a suite of software that extends OpenSHA (Field *et al.*, 2003; www.opensha.org) by adding loss-estimation capabilities. The calculator evaluates the following equation:

$$\mathrm{EAL} = \sum_{j=1}^{k} \mathrm{EAL}_j \qquad \mathrm{EAL}_j = \int_{s=0}^{\infty} V y(s) |G'(s)| ds, \tag{4}$$

where EAL denotes the expected annualized loss to the portfolio, j is an index to assets, EAL_j is the EAL for asset j, V is the replacement cost of a given asset, $y(s)$ is the expected value of loss (normalized by value) to asset j subjected to shaking s, $G(s)$ denotes the mean frequency (events per year) with which shaking s is exceeded at the location of asset j, and $G'(s)$ is its first derivative with respect to s. Equation (4) can be carried out numerically:

$$\begin{aligned} \mathrm{EAL}_j = V \sum_{i=1}^{n} \Bigg(& y_{i-1} G_{i-1} (1 - \exp(m_i \Delta s_i)) \\ & - \frac{\Delta y_i}{\Delta s_i} G_{i-1} \left(\exp(m_i \Delta s_i) \left(\Delta s_i - \frac{1}{m_i} \right) + \frac{1}{m_i} \right) \Bigg) \\ & \times V \sum_{i=1}^{n} (y_{i-1} a_i - \Delta y_i b_i), \end{aligned} \tag{5}$$

which is exact for a piecewise linear vulnerability function and piecewise loglinear hazard curve (Porter *et al.*, 2006). In equation (5), y_i more briefly denotes $y(s_i)$, G_i denotes $G(s_i)$, and

$$\begin{aligned} \Delta s_i &= s_i - s_{i-1} \\ \Delta y_i &= y_i - y_{i-1} \\ m_i &= \ln(G_i / G_{i-1}) / \Delta s_i \quad \text{for } i = 1, 2, \ldots n \\ a_i &= G_{i-1} (1 - \exp(m_i \Delta s_i)) \\ b_i &= \frac{G_{i-1}}{\Delta s_i} \left(\exp(m_i \Delta s_i) \left(\Delta s_i - \frac{1}{m_i} \right) + \frac{1}{m_i} \right). \end{aligned}$$

Vulnerability

One can estimate seismic vulnerability of a given structure type, denoted above by $y(s)$, various ways. Alternatives can be grouped as empirical (resulting from regression analysis

of earthquake experience data), analytical (from the application of engineering principles), or expert opinion. Steinbrugge (1982) and Wesson *et al.* (2004) are examples offering empirical vulnerability functions. ATC-13 is probably the U.S.'s leading example of seismic vulnerability functions drawn from expert opinion (Applied Technology Council [ATC], 1985). Some important milestones in the development of analytical seismic vulnerability functions include Czarnecki (1973), Kustu *et al.* (1982), Kircher *et al.* (1997), and various works recently establishing 2nd-generation performance-based earthquake engineering, for example, Beck *et al.* (1999), Porter *et al.* (2001), and Applied Technology Council (2012). We use three of these: one analytical, taken from FEMA's HAZUS-MH software (Porter, 2009), one empirical (Wesson *et al.*, 2004), and one based on expert opinion (ATC, 1985).

Portfolio EAL Calculator

HAZUS-MH could be used to calculate the desired EAL quantities, but it would involve substantial effort to generate shakemaps for each branch, import them, export results, and run the software for a large number of separate EAL calculations. To reduce this effort, the Portfolio EAL Calculator, rather than HAZUS-MH, was used to estimate EAL resulting from each branch of UCERF2. The calculator takes as input the portfolio data in a comma-separated-value text file with a header line and an arbitrary number of data lines. The header line is as follows:

AssetGroupName,AssetID,AssetName,BaseHt,Ded,
LimitLiab,Share,SiteName,Elev,Lat,Lon,Soil,ValHi,
ValLo,Value,VulnModel,V_{S30}

Subsequent data lines contain information about all buildings of the same type in the same location (here, census tract), organized in comma-separated columns below the header. Contents are detailed in Table 1.

The user selects UCERF2 parameter values and a GMPE, either via graphical user interface (Figure 5) or, as is the case here, via an XML file, the path to which is specified in another XML file. In the present application, the program calculates EAL for every allowable combination of UCERF2 parameter value and a specified GMPE. For average shearwave velocity in the upper 30 m of soil (V_{S30}), we used Wills and Clahan's (2006) map and that of Wald and Allen (2007). The intensity measures to be calculated are inferred from the vulnerability models, which specify how they measure *s*.

The calculator employs preexisting OpenSHA object classes to calculate site hazard for the selected parameter values and the first asset in the portfolio. It carries out the EAL calculations shown in equations (4) and (5) for that asset and sums over assets to estimate the portfolio EAL.

Table 1
Portfolio Contents

Field	Meaning	Type	Comment
AssetGroupName	Group name	Text	Non-unique name for group to which asset belongs, for example, "Houses"
AssetID	Asset identifier	Integer	A unique ID, for example, 1
AssetName	Asset name	Text	A label for the asset, for example, "House 1"
BaseHt	Reserved	Double	Reserved for later use
Ded	Ditto	Double	Ditto
LimitLiab	Ditto	Double	Ditto
Share	Ditto	Double	Ditto
SiteName	Site name	Text	A label for the site, for example, "769 N Michigan Ave, Pasadena CA 91104"
Elev		Double	Reserved for later use
Lat	Latitude	Double	Decimal degrees N, within ±90.00
Lon	Longitude	Double	Decimal degrees E, within ±180.00
Soil	NEHRP soil class	Text	NEHRP site soil classification, in {A, B, C, D, E, F}
ValHi	Upper bound of value at risk	Double	Value is uncertain or varies over time. Upper bound here is 97th percentile, ≥ value
ValLo	Lower bound value at risk	Double	Lower bound is 3rd percentile, ≤ Value
Value	Value at risk	Double	Best est. of value at risk, monetary or number or people, ≥ 0.00.
VulnModel	Vulnerability function	Text	Name of the vulnerability function to use for this asset, for example, "CUREE small house as-is," restricted to a list of available models
V_{S30}	Shearwave vel, m/sec	Double	Mean shearwave velocity in top 30 m of soil, m/sec, >0.00

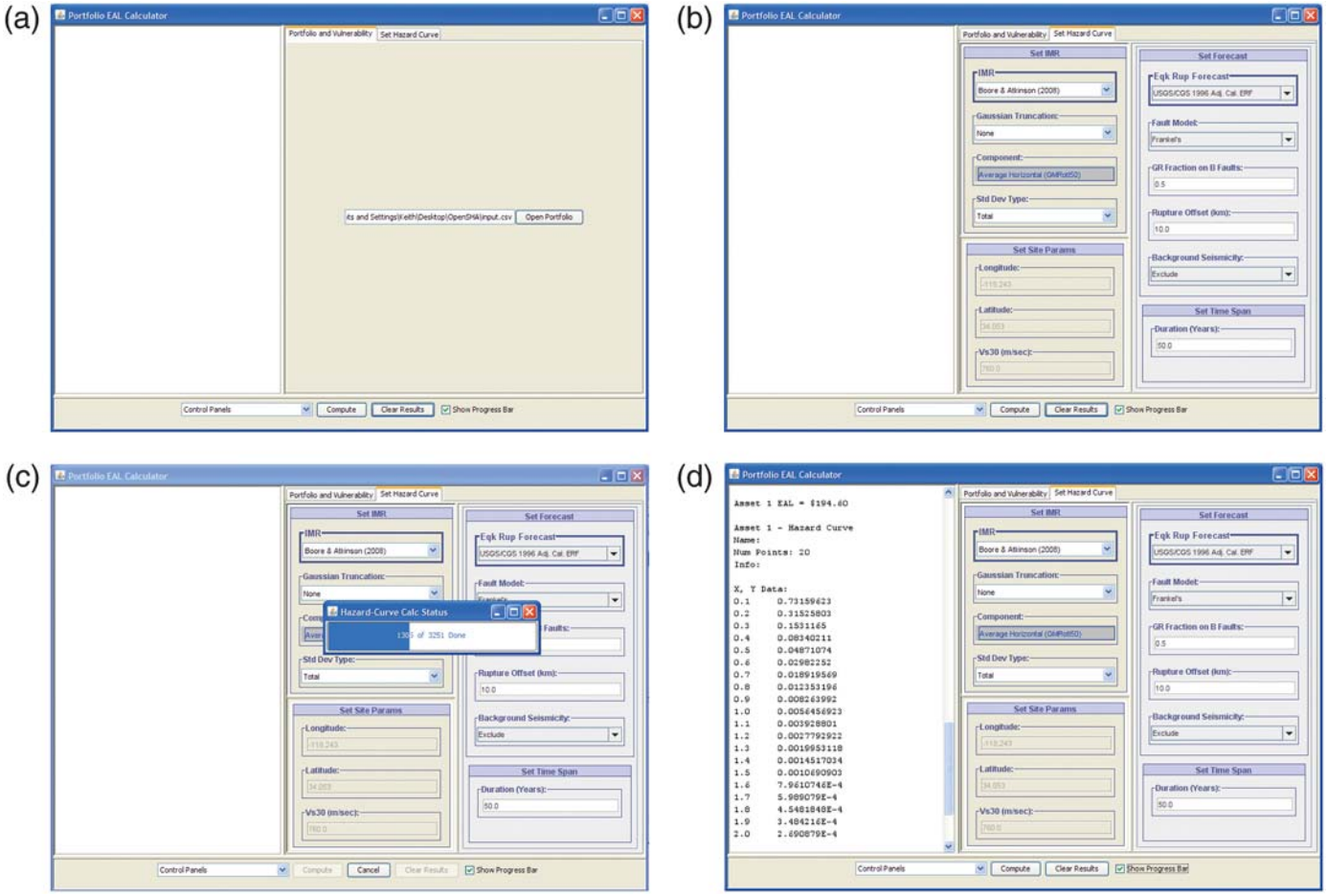

▲ **Figure 5.** Graphical user interface for the Portfolio EAL Calculator. The GUI allows one to specify parameter values for the earthquake rupture forecast, GMPE, timespan, and portfolio file. A command-line version was employed in the present study to loop over all branches of the UCERF2 logic tree.

Calculations for each asset are independent, conditioned on the model parameters, so the calculation is suited to parallel processing. The command-line Portfolio EAL Calculator takes advantage of this to distribute the calculations over a number of processors.

The calculations described here were performed at the High-Performance Computing Center of the University of Southern California (USC). The Center's Linux Computing Resource consists of 785 dual-core/dual-processor nodes and 5 × 16 processor, 64 GB, large memory servers, interconnected with Ethernet and 2GB Myrinet backbone, and a 1990 quad-core or hex-core/dual processor nodes cluster with Ethernet and a 10 GB Myrinet backbone. As of June 2012, USC's high-performance computing center ranks number 120 among the world's 500 fastest supercomputers (http://top500.org/list/2012/06/200).

With this hardware, the EAL calculations for 480 branches of the UCERF2 logic tree were performed in 24 batch jobs, each job handling 20 branches. Typically 5–10 jobs run concurrently. The job starts with the first branch. Each job has 40 processors available to it, distributed among five compute nodes, each with eight processors. The job distributes assets among processors. Individual processors compute EALs for their assets; these are summed to produce the portfolio EAL. The job then moves on to the 2nd branch and does the same thing until it has calculated portfolio EAL for its 20 branches.

Distributing the job this way, the calculation of EAL for a portfolio of 13,200 assets took approximately 30 min. These calculations reflect mapped faults only. Calculations of EAL from background sources were performed separately and added back in, because they do not vary by branch, but only by GMPE. Finally, results are reported via a text file. The file lists on each line the UCERF2 parameter values and the corresponding portfolio EAL, one record for each branch of the logic tree. Additional documentation of the Portfolio EAL Calculator can be found at www.opensha.org.

Construction of the tornado diagram required modifying the methodology described earlier. Most of the branches are uncertain nominal values, which have no associated order, let alone 10th or 90th percentile values. We can assign probabilities to them in the Bayesian sense (probability as degree of belief), but not order; only ordinal and cardinal numbers have

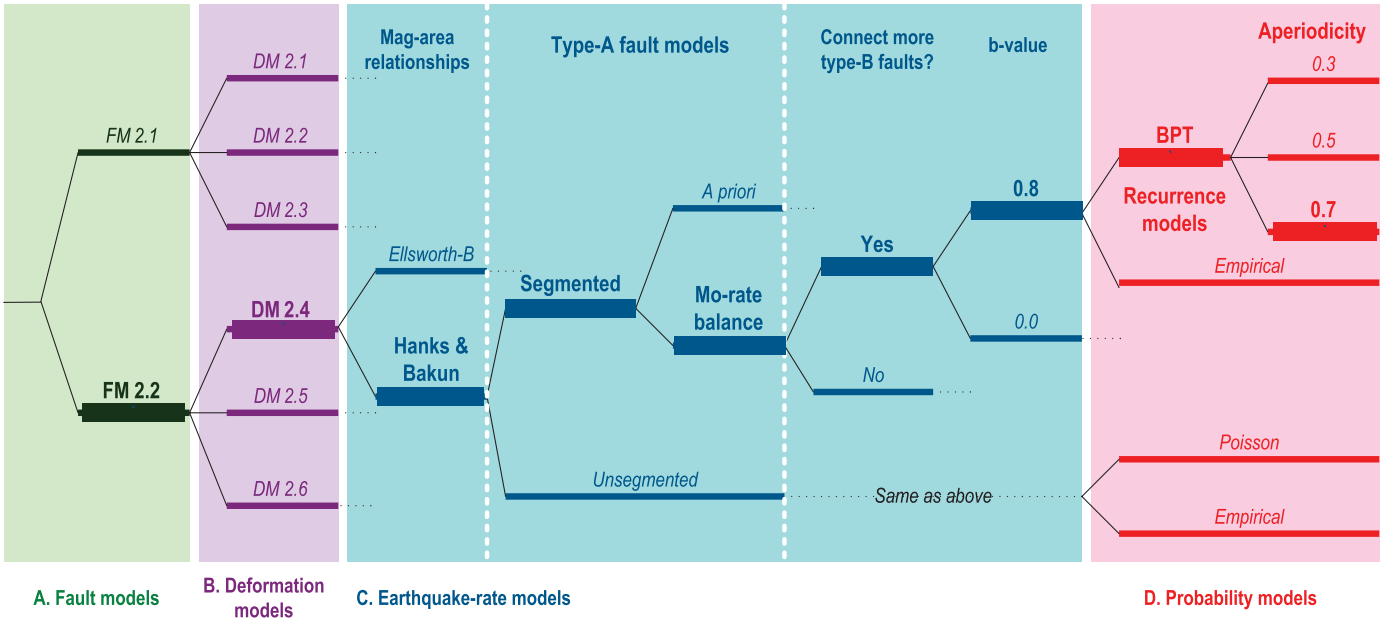

▲ **Figure 6.** Baseline branch of the logic tree shown in bold. Baseline GMPE is Chiou and Youngs (2008).

that property. So the baseline values are selected from the branch that produces the 960th largest value of EAL, among all 1920 samples.

RESULTS

The Portfolio EAL Calculator estimated EAL for 1920 branches: each of the 480 branches of the UCERF2 earthquake rate model, and each of four NGA equations (Chiou and Youngs, 2008; Campbell and Bozorgnia, 2008; Boore and Atkinson, 2008; Abrahamson and Silva, 2008). Branches are sorted in increasing order of EAL. The baseline branch is selected as the 960th in the sorted list. Results are not especially sensitive to which particular values of the uncertainties appear on the baseline branch. Note that, conditioned on a single branch of the logic tree, EAL has a single deterministic value, the integral of loss and the absolute value of the first derivative of exceedance frequency. Let us refer to this value as the conditional EAL. When viewed from the perspective of the full UCERF2 logic tree, the conditional EAL is uncertain, and has a probability distribution.

Using the HAZUS-MH vulnerability models from Porter (2009) and the Wills and Clahan (2006) V_{S30} model, the minimum EAL value among 1920 branches was \$0.64 billion; the value exceeded by 50% of branches (median in terms of order) was \$1.22 billion; the maximum was \$2.05 billion. The minimum, baseline, and maximum values represent \$0.40, \$0.76, and \$1.27 per \$1000 of exposed value (a common way to normalize losses against exposed value). The median or baseline branch is illustrated in Figure 6; parameter values producing low, median, and high values are shown in Table 2.

The weighted-average of the conditional EAL of all 1920 branches—weights from Figure 1—is \$1.21 billion, which almost equals the baseline EAL of \$1.22 billion. The standard deviation is \$0.30 billion, indicating a coefficient of variation of 0.25, and that the extrema are approximately −1.9 and +2.7 standard deviations from the baseline, equivalent to approximately 3% and 99.7% bounds for a Gaussian distribution, which seems reasonable.

The tornado diagram's parameter values are shown in Table 3. The diagram is shown in Figure 7. It reflects 19 branches including the baseline, and has only slightly narrower EAL extrema than all 1920 branches, an important point discussed later.

Figure 7 suggests that the choice of recurrence model, aperiodicity in the BPT recurrence model, and GMPE are

Table 2
Parameter Values Producing Low, Baseline (Median in Terms of Order), and High EAL Values

Order	Def mod	Mag–area	A-Fault Solution	Rates	Connect More B Faults?	*b*	Recurrence	Aperiodicity	GMPE	EAL, \$B
Min	D2.4	Hanks-Bakun	Segmented	Mo-rate bal	Yes	0.0	Empirical		CY08	\$0.64
Med	D2.4	Hanks-Bakun	Segmented	Mo-rate bal	Yes	0.8	BPT	0.7	CY08	\$1.22
Max	D2.2	Hanks-Bakun	Segmented	Mo-rate bal	No	0.8	BPT	0.3	AS08	\$2.05

Table 3
Results Used to Create Tornado Diagram

Parameter	Parameter Value Associated with		Expected Annualized Loss ($B)		
	Low EAL	High EAL	Low EAL	High EAL	Swing
Recurrence model	Empirical	BPT (0.5)	0.76	1.33	0.57
Ground-motion-prediction equation	CB2008	AS2008	1.21	1.51	0.30
Fault-slip rates	Mo-rate balance	A priori	1.20	1.22	0.02
Magnitude-area	Ellsworth-B	Hanks-Bakun	1.02	1.22	0.20
Connect more B-faults?	TRUE	FALSE	1.22	1.27	0.05
Def model	D2.6	D2.2	1.22	1.25	0.03
A-Fault solution	Unsegmented	Segmented	1.11	1.22	0.11
B-fault *b*-value	0	0.8	1.21	1.22	0.01

the leading sources of uncertainty in the estimate of EAL among California woodframe single-family dwellings, followed by the choice of which magnitude–area relationships to use. Less important to this metric are the method for estimating type-A fault rupture rates (*a-priori* or moment-balanced models), the question of whether to connect more Type-B faults, the choice of deformation model, the question of whether to enforce segmentation on Type-A faults, and the choice of b-value to Type-B faults.

The trimmed logic tree is shown in Figure 8. Considering only its 40 branches, the expected value and coefficient of variation (COV) of the conditional EAL are $1.17B and 0.25 respectively, almost the same as the full 1920-branch tree. By contrast, if one fixes the recurrence model, aperiodicity, magnitude–area relationship, and GMPE at their baseline values, the expected value and COV of EAL are $1.23B and 0.024 respectively; the COV considering all uncertainties except the key ones is 1/10th that of the full 1920-branch set. Table 4 recapitulates these figures.

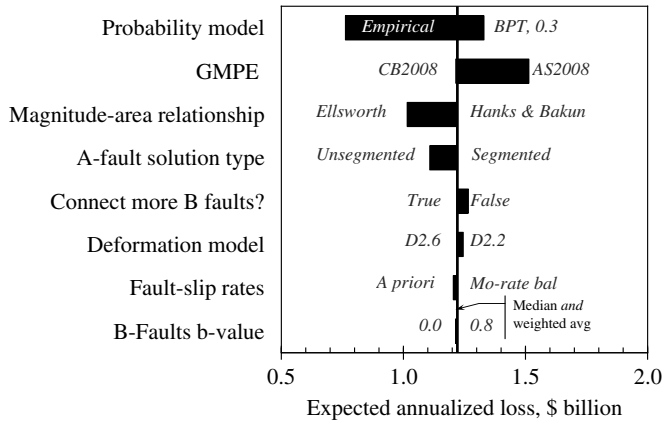

▲ **Figure 7.** Effect of UCERF2 and ground-motion-prediction equation (GMPE) branches on EAL. Note that the line labeled "weighted average of 1920 branches" uses the weights in Figure 1, the EAL values calculated for each branch, and is so close to the baseline EAL that it is indistinguishable in this figure.

That the trimmed tree produces approximately the same probability distribution as the full tree is illustrated in Figure 9, which shows that the two EAL distributions pass a Kolmogorov–Smirnov goodness-of-fit test at the 5% significance level. This suggests that one can accept the hypothesis that the two distributions are drawn from the same population. It seems reasonable to conclude, therefore, that the tornado diagram accurately identifies the branches that matter.

We tested the sensitivity of the tornado-diagram results to the choice of baseline values by performing the analysis again using the values in the 963rd record as the baseline instead of the values in the 960th. The two baselines differ in their ground-motion-prediction equation, deformation model, magnitude–area relationship, aperiodicity, B-fault *b*-value, and in whether to connect more B-faults. Figure 10 compares the two tornado diagrams. Although the 2nd and 3rd most-important variables switch order, both diagrams pick out the same key uncertainties (the ones that matter most to the uncertainty in EAL), which is the central objective of the tornado-diagram analysis.

DISCUSSION

Why Does Figure 7 Look Different From Figure 4?

The bars in Figure 7 end at the baseline rather than crossing it, as in Figure 4, because Figure 4 tests the sensitivity of loss mostly to scalar continuous random variables, each of which has a median value. The baseline in Figure 4 runs through those median values. The variables in Figure 7 are mostly nominal, meaning they can only take on a few discrete values and those values have no order. For example, there are only two possible magnitude–area relationships, Ellsworth-B or Hanks and Bakun (2008), and no order or median value *per se*. The baseline in Figure 7 has therefore been taken as the EAL from the branch that produces the 960th largest of 1920 EAL values, not the EAL produced by taking the median values for each variable.

What About Interaction Between Variables?

There is some interaction between variables, but it is not strong. The minimum and maximum EAL values considering

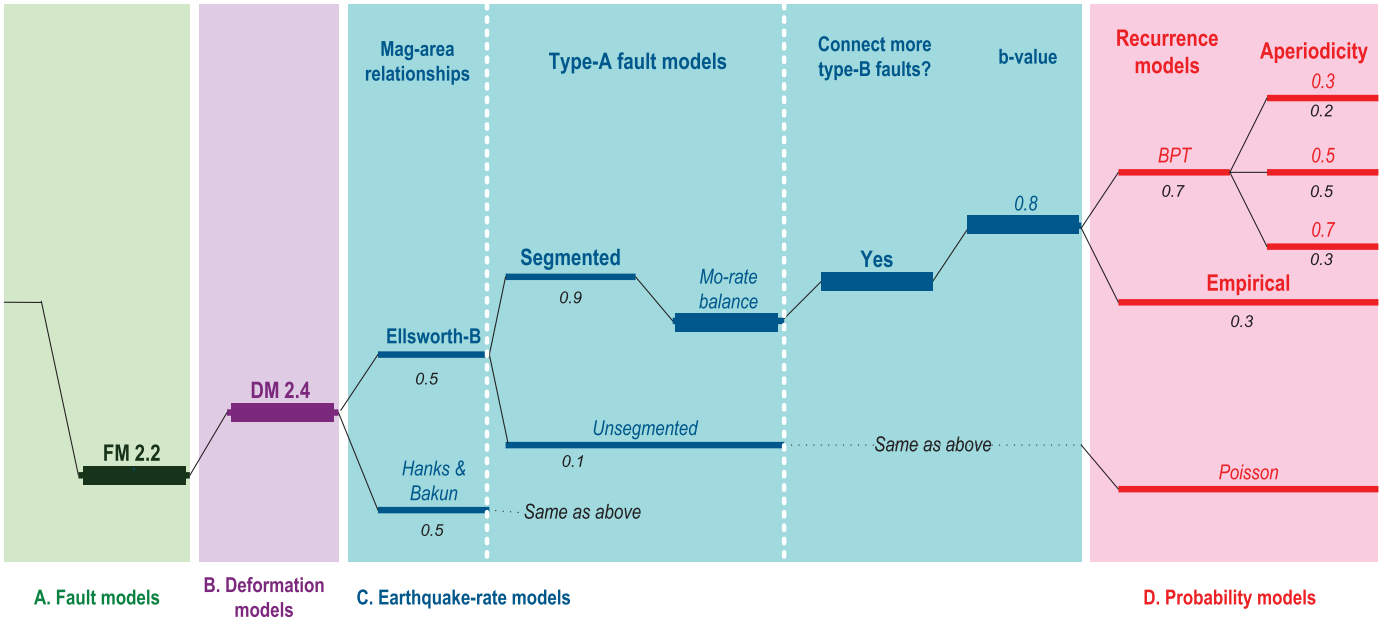

▲ **Figure 8.** Trimmed UCERF2 logic tree. It has 10 branches, including the ones that lead from the Hanks & Bakun magnitude–area relationship. Not shown are the four ground-motion-prediction equations which, when combined with the 10 UCERF2 branches, make 40.

all 1920 branches are close to the extrema of the bars in the tornado diagram. The variables can combine to produce EALs that are more extreme, but not much more extreme.

What About Other Variables, Such As Vulnerability, V_{S30}, and the Portfolio?

Results are not strongly sensitive to the choices of vulnerability model or V_{S30}. We performed the analysis using Wald and Allen's V_{S30} map, and then again with the ATC-13 vulnerability function, and finally with that of Wesson *et al.* (2004), both with Wills and Clahan's (2006) V_{S30} values. We also analyzed a portfolio comprising almost all of the California building stock.

The results are shown in Figure 11. Though the baseline values vary modestly ($1.09, $1.28, and $1.07 billion for ATC-13, Wesson, and Wald–Allen respectively, versus $1.22 billion for HAZUS-based vulnerability functions), the diagrams show essentially the same results: the probability model, magnitude–area relationship, and GMPE dominate the uncertainty; the order of the variables in the diagram is generally the same, and the branches that produce the minima and maxima are largely unchanged. The baseline for the statewide portfolio is $1.50 billion, reflecting the larger exposed value. The weighted-average EAL from all 1920 branches for the ATC-13, Wesson, Wald–Allen, and all-building models are $1.07, $1.31, $1.05, and $1.47 billion, close to the baseline figures of $1.09, $1.28, $1.07, and $1.50 billion respectively. Overall coefficients of variation in the four cases are 0.26, 0.30, 0.26, and 0.27, respectively, all approximately the same as using the HAZUS-MH-based vulnerability functions and Wills and Clahan (2006) V_{S30} map.

One can perform some modest validation of these results by comparing the EAL figures with values produced using different models. The normalized figure of $0.76 per $1000 compares well with FEMA 366's estimate of $3.5 billion EAL, which divided by $4.4 trillion total exposed value (building and contents), equals $0.79 per $1000 (Federal Emergency Management Agency [FEMA], 2008). The California Earthquake Authority (2011) estimates its own EAL as of December 2010 to be $217 million on exposure of $274 billion, equivalent to $0.76 per $1000 (after deductibles and limits). One can also estimate California's actual loss history in the years

Table 4
Mean and Standard Deviation of Conditional EAL for Full Original Tree, Trimmed Tree, and the Branches Eliminated by the Trimming Process. The Last of These Uses the Baseline Values for Recurrence Model, Aperiodicity, Magnitude-area Relationship, and Ground-Motion-Prediction Equation, and Allow All Other Uncertainties to Vary

	Full tree	Trimmed tree	Eliminated branches
Mean	$ 1.21	$ 1.17	$ 1.23
Coefficient of variation	0.25	0.25	0.02

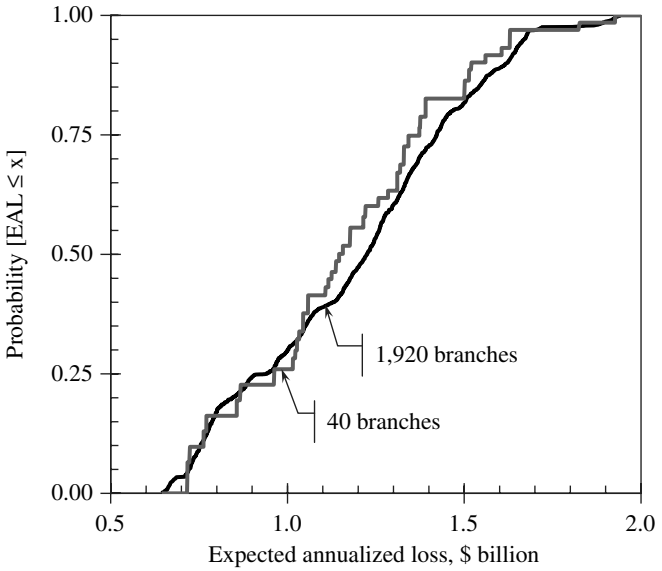

▲ **Figure 9.** Kolmogorov–Smirnov test suggests that 40-branch trimmed logic tree and full 1920-branch logic tree draw from the same population.

1965–2005 by dividing the $58.5 billion in total estimated losses during that period (Rowshandel *et al.*, 2003; year-2000 dollars) by 40 years and an average total exposed building value of say $2.0 trillion (the present estimate of building value reduced to account for population growth), yielding an approximate EAL of $0.73 per $1000. That the recurrence model is a key uncertainty, is also supported by Field *et al.* (2009), who examined the sensitivity of the UCERF2 model to its various branches. Considering the rate at which events of $M \geq 6.7$ occur, they found that "The empirical versus BPT/Poisson probability-model branch is by far the most influential in our logic tree."

We can also check our findings considering sample sites. Statewide risk is probably heavily influenced by the Los Angeles and San Francisco Bay areas. As representative and interesting sites, we chose the Southern California Earthquake Center (SCEC) at the University of Southern California, and the Oakland address of the Earthquake Engineering Research Institute (EERI). With geolocations from Google Earth, V_{S30} from Wills and Clahan (2006), and depth to bedrock from the SCEC Community Velocity Model, parameter values are:

USC: 34.023N 118.286W; $V_{S30} \approx 280$ m/sec; depth to 1.0 km/sec = 0.5 km; to 2.5 km/sec = 3.5 km
EERI: 37.804N 122.273W; $V_{S30} \approx 302$ m/sec; depth to 1.0 km/sec = 0.13 km; to 2.5 km/sec = 0.87 km

Hazard curves for each site are calculated using the OpenSHA Hazard Curve Calculator (local, version 1.2.3). Hazard is measured here in terms of Sa(0.3 sec, 5%). It is calculated under baseline conditions, and varying them from baseline one at a time, high or low aperiodicity (0.7 and 0.3), empirical or BPT (aperiodicity = 0.5) probability models, extreme GMPEs, and indicated fault-slip-rate alternatives (see Fig. 12). We focus on shaking with 2% exceedance probability in 1 year ("50-year shaking"), in the recurrence frequency range that tends to dominate EAL. Sensitivity of 50-year shaking at the two sites to the various uncertainties tends to mirror that of the portfolio as a whole: recurrence model and GMPE making a big difference, moment-area and fault slip rate models making much less difference.

We also examined losses more closely for 10 sample California sites in the portfolio. Sites were selected at random in a stratified sample, where each stratum had equal cumulative value (10% of the total), and each site within a stratum had equal likelihood of being selected. The sample is shown in Table 5. Each site represents all construction of the specified type in the specified census tract. Mean loss was calculated for each site given mean shaking for each of approximately 12,000

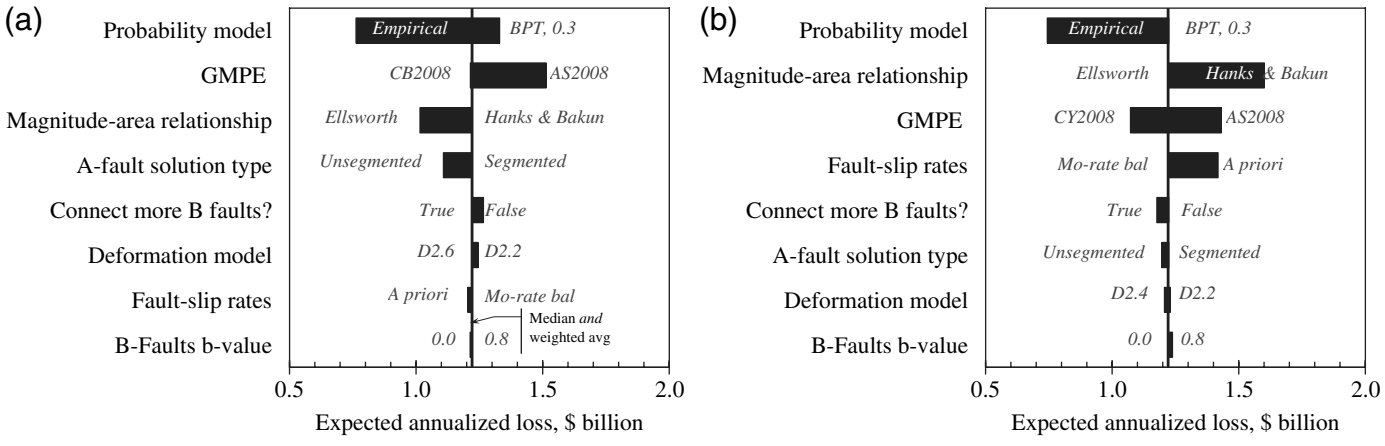

▲ **Figure 10.** Results are not very sensitive to baseline values: (a) shows the tornado diagram based on the 960th record in the sorted list of EAL; (b) shows the diagram based on the 963rd, which differs in baseline ground-motion-prediction equation, deformation model, magnitude–area relationship, aperiodicity, B-fault *b*-value, and in whether to connect more B-faults.

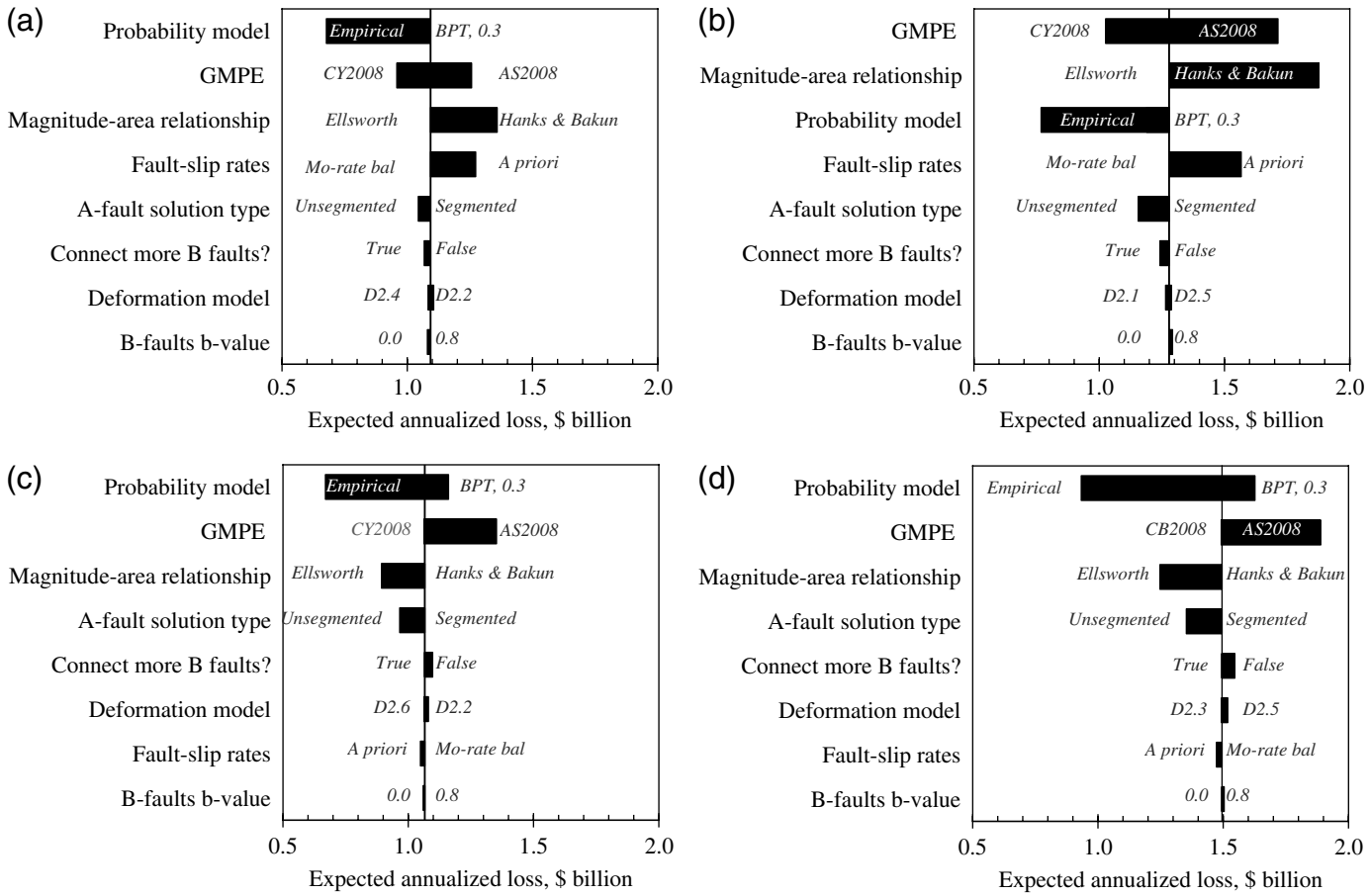

▲ **Figure 11.** UCERF2 tornado diagrams using (a) ATC-13 (b) Wesson *et al.* vulnerability models (c) Wald and Allen (2007) V_{S30} and (d) a statewide inventory of all buildings.

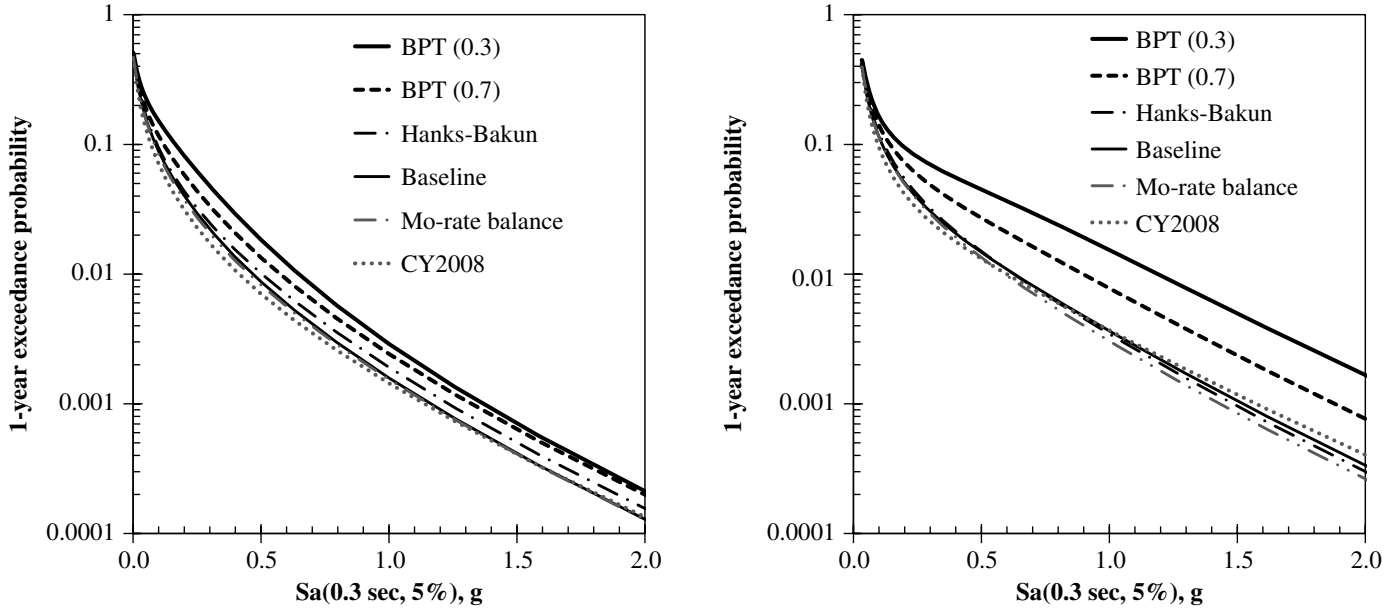

▲ **Figure 12.** Sensitivity of hazard at USC (left) and EERI (right) to UCERF2 epistemic uncertainties. Hazard for these two sites approximately tracks sensitivity of EAL to the uncertainties indicated by the tornado diagram. Sa refers to damped elastic spectral acceleration response at the stated period and damping ratio.

Table 5
Sample Portfolio for Deaggregating Loss and Testing Effect of GMPE

Lat N	Lon E	V_{S30} (m/sec)	Replacement Cost ($000)	Structure Type
34.0469	−118.2617	280	$ 603	W1-m-RES1-DF
33.8781	−118.1600	280	$ 16,044	W1-h-RES1-DF
36.8444	−119.7923	387	$ 22,602	W1-h-RES1-DF
34.2455	−118.4176	280	$ 33,369	W1-h-RES1-DF
37.8455	−122.2836	280	$ 35,306	W1-h-RES1-DF
34.0557	−118.3706	280	$ 35,881	W1-h-RES1-DF
34.8860	−120.4251	349	$ 139,017	W1-h-RES1-DF
33.6094	−117.6852	390	$ 150,521	W1-h-RES1-DF
33.8808	−118.4073	387	$ 219,850	W1-m-RES1-DF
37.5482	−121.9499	280	$ 351,695	W1-m-RES1-DF

ruptures, using the OpenSHA event-set calculator (www.opensha.org).

Weighting by contribution to the portfolio EAL, the weighted-average V_{S30} of the sites is 330 m/sec, the Joyner-Boore distance is 27 km, and the magnitude is 7.05. Referring to Figure 2, these parameters suggest 20%–30% uniformly higher mean shaking under AS2008 than CY2008, i.e., 0.25 g versus 0.20 g. At these shaking intensities, mean repair cost, assuming AS2008, is approximately 75% higher than under CY2008, because of nonlinearity in the vulnerability functions. This is more than enough to account for the 50% greater portfolio EAL under AS2008 than CY2008.

The data presented here show that the other epistemic uncertainties contribute little to uncertainty in statewide EAL, but they do not explain why. We can hypothesize (though this study stops short of testing the hypotheses): it seems reasonable that parameters associated with Type-B faults should not strongly influence EAL because, almost by definition, most are smaller and less active than Type-A faults and therefore contribute less to hazard at the statewide level. That the deformation model does not strongly affect statewide hazard also seems reasonable, since the differences between the models have to do with allocating the same slip between two faults. Reductions in the contribution to EAL resulting from lower slip rates on one fault would be offset by increases resulting from higher slip rates on the other.

Several questions remain. UCERF2 will be replaced with version 3, currently under development; we do not know how the findings will change. UCERF3 aims to include multi-fault ruptures and spatiotemporal clustering. The NGA relationships are also undergoing an update and, again, we do not know how this will affect the findings. We do not know how the tornado diagram might differ if, instead of EAL, we examined a large rare loss (such as the loss with 0.4% exceedance probability in a year, often referred to as probable maximum loss, or PML), or loss measured in terms of casualties rather than repair costs. We do not know the extent to which an examination of insurance loss (which includes deductibles and limits) might produce different results. We have only partially examined why the epistemic uncertainties in UCERF2 have the relative impact suggested here. We have not examined how the findings might differ if one examined a portfolio from a small region, such as a city in southern California. We do not know the extent to which taking weighted averages of certain branches, such as the GMPEs, might underestimate uncertainty. And we offer no opinion on the relative scientific importance of resolving any of the uncertainties.

CONCLUSIONS

There are many ways to explore the relative importance of the various modeling uncertainties of the UCERF2 earthquake rupture forecast (WGCEP, 2007) for the state of California. We set out to better understand which uncertainties matter most to societal economic risk, and performed a tornado-diagram analysis of the sensitivity of EAL experienced by an estimated statewide portfolio of woodframe single-family dwellings. Here, EAL refers to expected value of repair cost for the buildings alone.

We estimated EAL for 1920 combinations of UCERF2 modeling choice (480 branches) and four NGA relationships, using a program we created called the Portfolio EAL Calculator, an extension of the OpenSHA software. The tornado-diagram analysis shows that the uncertainty in the EAL among all California woodframe single-family dwellings is dominated by the choice of recurrence model; the aperiodicity parameter value; the choice of ground-motion-prediction equation, and the choice of magnitude–area relationship. They represent 40 of the 1920 branches when one fixes all the others at a value arbitrarily selected from the available options.

Treating EAL as a random variable that varies with UCERF2 modeling choices and GMPE, two probability distributions of EAL were calculated: one considering all 1920 branches and another where only the key uncertainties vary. The two distributions have the same mean and coefficient of variation, and pass a Kolmogorov–Smirnov goodness-of-fit test, which suggests they come from the same underlying distribution. The remaining epistemic uncertainties, while scientifically important and potentially material to local seismic hazard, local seismic risk, and perhaps low-probability,

high-loss events, only modestly affect statewide EAL experienced by single-family woodframe dwellings or by the statewide building stock as a whole.

One implication is that, if one is examining statewide EAL and wishes to save computational time, the top three epistemic uncertainties alone sufficiently represent uncertainty in hazard. Considering them alone would reduce the complexity of the logic tree by 50 times, from 1,920 to 40 branches. The 40 branches comprise five combinations of recurrence model and aperiodicity (counting "empirical" only once among recurrence models), four ground-motion-prediction equations, and two magnitude–area relationships. The reduction in model complexity and computation effort is not accompanied by a loss in uncertainty or a bias in expectation, compared with a model that considers all 1,920 branches.

Another implication is that, for a user of risk information concerned with statewide EAL, gathering more knowledge of any of the key epistemic uncertainties could be more effective in reducing uncertainty than exploring the other sources of uncertainty. These conclusions are unchanged if one uses either the leading expert-opinion-based alternative vulnerability model (ATC-13) or a recent empirical one (Wesson *et al.*, 2004), or if one uses an alternative model of V_{S30}, namely Wald and Allen (2007), or if one uses a statewide portfolio representing all buildings rather than just woodframe single-family dwellings.

A number of questions remain, such as how these findings might differ under UCERF3, or using PML, casualties, or insurance EAL instead of ground-up EAL as the risk metric.

ACKNOWLEDGMENTS

This research was supported by the Southern California Earthquake Center. SCEC is funded by NSF Cooperative Agreement EAR-0106924 and USGS Cooperative Agreement 02HQAG0008. Computation for the work described in this paper was supported by the University of Southern California Center for High-Performance Computing and Communications (www.usc.edu/hpcc). Any use of trade, firm, or product names is for descriptive purposes only, and does not imply endorsement by the U.S. Government.

REFERENCES

Abrahamson, N., and W. Silva (2008). Summary of the Abrahamson & Silva NGA ground-motion relations, *Earthquake Spectra* **24,** no. 1, 67–97.

Akinci, A., F. Galadini, D. Pantosti, M. Petersen, L. Malagnini, and D. Perkins (2009). Effect of time-dependence on probabilistic seismic hazard maps and deaggregation for the Central Apennines, Italy, *Bull. Seismol. Soc. Am.* **99,** no. 2A, 585–610, http://www.bssaonline.org/content/99/2A/585 (last accessed December 2011).

American Society of Civil Engineers (ASCE) (2005). *Minimum Design Loads for Buildings and Other Structures, SEI/ASCE 7-05*, Reston, Virginia.

American Society of Civil Engineers (2010). *Minimum Design Loads for Buildings and Other Structures, SEI/ASCE 7-10*, Reston, Virginia, 608 pp .

Applied Technology Council (ATC) (1985). *ATC-13, Earthquake Damage Evaluation Data for California*, Redwood City, California, 492 pp.

Applied Technology Council (ATC), (2012). *ATC-58: Guidelines for Seismic Performance Assessment of Buildings, 100% Draft*. Redwood City, California.

Beck, J. L., A. Kiremidjian, S. Wilkie, A. Mason, T. Salmon, J. Goltz, R. Olson, J. Workman, A. Irfanoglu, and K. Porter (1999). *Decision Support Tools for Earthquake Recovery of Businesses, Final Report*, CUREE-Kajima Joint Research Program Phase III, Consortium of Universities for Earthquake Engineering Research, Richmond, California.

Boore, D. M., and G. M. Atkinson (2008). Ground-motion prediction equations for the average horizontal component of PGA, PGV, and 5%-damped PSA at spectral periods between 0.01 s and 10.0 s, *Earthquake Spectra* **24,** no. 1, 99–138.

California Earthquake Authority (2011). *Governing Board Memorandum, June 30, 2011, Second Annual Risk-Capital Surcharge for Safeco Insurance Company of America*, Sacramento, California, 2 pp.

Campbell, K. W., and Y. Bozorgnia (2008). NGA ground motion model for the geometric mean horizontal component of PGA, PGV, PGD and 5% damped linear elastic response spectra for periods ranging from 0.01 to 10 s, *Earthquake Spectra* **24,** no. 1, 139–171.

Chiou, B. S. J., and R. R. Youngs (2008). An NGA model for the average horizontal component of peak ground motion and response spectra, *Earthquake Spectra* **24,** no. 1, 173–216.

Cornell, C. A., and E. H. Vanmarcke (1969). The major influences on seismic risk, *Proc. Fourth World Conf. Earthquake Eng.*, A1–69 to A1–83.

Czarnecki, R. M. (1973). *Earthquake Damage to Tall Buildings*, Structures Publication 359, Massachusetts Institute of Technology, Cambridge, Massachusetts, 125 pp.

Federal Emergency Management Agency (FEMA) (2008). *FEMA-366b: HAZUS-MH Estimated Annualized Earthquake Losses for the United States*, Washington, DC, 53 pp.

Field, E. H., T. H. Jordan, and C. A. Cornell (2003). OpenSHA: A developing community-modeling environment for seismic hazard analysis, *Seismol. Res. Lett.* **74,** no. 4, 406–419.

Field, E. H., T. E. Dawson, K. R. Felzer, A. D. Frankel, V. Gupta, T. H. Jordan, T. Parsons, M. D. Petersen, R. S. Stein, R. J. Weldon II, and C. J. Wills (2009). Uniform California earthquake rupture forecast, version 2 (UCERF 2), *Bull. Seismol. Soc. Am.* **99,** no. 4, 2053–2107.

Grossi, P. (2000). Quantifying the uncertainty in seismic risk and loss estimation, in *Proc. of the EuroConference on Global Change and Catastrophe Risk Management: Earthquake Risks in Europe, IIASA*, Laxenburg, Austria, 6–9 July 2000, http://www.iiasa.ac.at/Research/RMS/july2000/Papers/grossi.pdf (last accessed December 2011).

Hanks, T. C., and W. H. Bakun (2008). *M*-log A observations for recent large earthquakes, *Bull. Seismol. Soc. Am.* **98,** 490–494.

Kircher, C. A., A. A. Nassar, O. Kustu, and W. T. Holmes (1997). Development of building damage functions for earthquake loss estimation, *Earthquake Spectra* **13,** no. 4, 663–682.

Kustu, O., D. D. Miller, and S. T. Brokken (1982). *Development of Damage Functions for Highrise Building Components*, For the US Department of Energy, URS/John A Blume & Associates, San Francisco, California.

Multihazard Mitigation Council (MMC) (2005). *Natural Hazard Mitigation Saves: An Independent Study to Assess the Future Savings from Mitigation Activities*, National Institute of Building Sciences, Washington, D.C..

National Institute of Building Sciences and Federal Emergency Management Agency (NIBS and FEMA) (2009). *Multi-hazard Loss Estimation Methodology, Earthquake Model, HAZUS®MH MR4 Technical Manual*, Federal Emergency Management Agency, Washington, D.C..

Porter, K. A. (2009). Cracking an open safe: more HAZUS vulnerability functions in terms of structure-independent spectral acceleration,

Earthquake Spectra **25,** no. 3, 607–618, http://www.sparisk.com/pubs/Porter-2009-Safecrack-MDF.pdf (last accessed July 2012).

Porter, K. A., J. L. Beck, and R. V. Shaikhutdinov (2002). Sensitivity of building loss estimates to major uncertain variables, *Earthquake Spectra* **18,** no. 4, 719–743, http://www.sparisk.com/pubs/Porter-2002-Sensitivity.pdf (last accessed July 2012).

Porter, K. A., A. S. Kiremidjian, and J. S. LeGrue (2001). Assembly-based vulnerability of buildings and its use in performance evaluation, *Earthquake Spectra*, **17,** no. (2), 291–312, http://www.sparisk.com/pubs/Porter-2001-ABV.pdf (last accessed July 2012).

Porter, K. A., and C. R. Scawthorn (2007). *OpenRisk: Open-Source Risk Estimation Software*, SPA Risk, Pasadena, California, 107 pp., http://www.sparisk.com/pubs/SPA-2007-OpenRisk.pdf (last accessed July 2012).

Porter, K. A., and C. R. Scawthorn (2009). *Development of Open Source Seismic Risk Modeling Framework*, *Rept. to the U.S. Geol. Surv. under award no 07HQAG0002*, SPA Risk LLC, Denver, Colorado, www.sparisk.com/pubs/SPA-2009-OpenRisk.pdf (last accessed July 2012).

Porter, K. A., C. R. Scawthorn, and J. L. Beck (2006). Cost-effectiveness of stronger woodframe buildings, *Earthquake Spectra* **22,** no. 1, 239–266, http://www.sparisk.com/pubs/Porter-2006-woodframe.pdf (last accessed July 2012).

Rabinowitz, N., D. M. Steinberg, and G. Leonard (1998). Logic trees, sensitivity analyses, and data reduction in probabilistic seismic hazard assessment, *Earthquake Spectra* **14,** no. 1, 189–201.

Rowshandel, B., M. Reichle, C. Wills, T. Cao, M. Petersen, D. Branum, and J. Davis (2003). Estimation of future earthquake losses in California. in *Proc. Am. Geophys Union, Fall Meeting 2003*, San Francisco California, December 2003.

Steinbrugge, K. V. (1982). *Earthquakes, Volcanoes, and Tsunamis, an Anatomy of Hazards*, Skandia America Group, New York, 392 pp.

Wald, D. J., and T. I. Allen (2007). Topographic slope as a proxy for seismic site conditions and amplification, *Bull. Seismol. Soc. Am.* **97,** 1379–1395.

Working Group on California Earthquake Probabilities (WGCEP) (2007). *The Uniform California Earthquake Rupture Forecast, Version 2 (UCERF 2), U.S. Geol. Surv. Open-File Rept. 2007-1437 and California Geol. Surv. Special Rept. 203*, http://pubs.usgs.gov/of/2007/1437/ (last accessed December 2011).

Wesson, R. L., D. M. Perkins, E. V. Leyendecker, R. J. Roth, and M. D. Petersen (2004). Losses to single-family housing from ground motions in the 1994 Northridge, California, Earthquake, *Earthquake Spectra* **20,** no. 3, 1021–1045.

Wills, C. J., and K. B. Clahan (2006). Developing a map of geologically defined site-conditions categories for California, *Bull. Seismol. Soc. Am.* **96,** no. 4A, 1483–1501.

Youngs, R. R., and K. J. Coppersmith (1985). Implications of fault slip rates and earthquake recurrence models to probabilistic seismic hazard estimates, *Bull. Seismol. Soc. Am.* **75,** no. 4, 939–964.

Keith A. Porter
SPA Risk LLC
2501 Bellaire Street
Denver, Colorado 80207 U.S.A.
keith@cohen-porter.net

Edward H. Field
U.S. Geological Survey
P.O. Box 25046
Mail Stop 966
Golden, Colorado 80225-0046 U.S.A.

Kevin Milner
University of Southern California
Southern California Earthquake Center
3651 Trousdale Parkway, Room 169
Los Angeles, California 90089 U.S.A.